Electronic Supplementary Material (ESI) for Dalton Transactions.

Supporting Information:

MoC as an effective co-catalyst for $MAPbI_3$ photo-catalysis HI for hydrogen evolution

Tiantian Zhang, Jianfei Yu, Jiyao Huang, Shengnan Lan, Yongbing Lou*, Jinxi Chen*

School of Chemistry and Chemical Engineering, Jiangsu Engineering Laboratory of Smart Carbon-Rich Materials and device, Southeast University, Nanjing 211189, PR China.

* Corresponding author.

E-mail: chenjinxi@seu.edu.cn

Chemicals:

All reagents were used without any purification. PbI_2 (Lead(Ⅱ) Iodide, 99%, Aldrich), hydroiodic acid (HI, 57 wt% in water, Aladdin), methylamine (CH_3NH_2, 30 wt% in absolute ethanol, Aladdin), hypophoaphoeous acid (H_3PO_2, 50 wt% in water, Aladdin), ammonium molybdate($(NH_4)_6Mo_7O_{24}\cdot 4H_2O$, Aladdin), dicyandiamide($C_2H_4N_4$, XIYA Reagent)

Synthesis of MAI:

Under ice water bath, add 20 ml HI solution and 45 ml CH_3NH_2 ethanol solution to a beaker and stir for two hours; then transfer the solution to a rotary evaporator and evaporate to dryness at 60 °C. The obtained solid powder is dissolved in absolute ethanol Recrystallize with anhydrous ether. This process is repeated three times and a white powder will be obtained. Dry in a vacuum drying oven at 60 °C for ten hours to obtain white MAI powder.

Synthesis of Pt/$MAPbI_3$:

$MAPbI_3$/Pt composites were achieved by photodeposition. Specifically, 49 mg of $MAPbI_3$ and 1 mg of $H_2PtCl_6\cdot 6H_2O$ were added to the preprepared $MAPbI_3$ saturated solution, which was sonicated for 20 min and stirred for another 30 min to obtain the homogeneous mixture. The suspension was then exposed to visible light produced by a Xe lamp with a 420 nm cutoff filter and photodeposited in an Ar atmosphere for 2 h. The entire process was maintained at 15 °C via a cooling water system.

Characterization:

The Zeta potential of the sample was measured using a multi-angle particle size potential analyzer, the instrument model is Nanobrook Omni. Sample preparation method: the sample is dispersed in HI solution through ultrasonic treatment, and then the suspension is put in the sample pool for testing. X-ray diffraction (XRD) measurements with an incident radiation Cu Kα (λ = 0.15406 nm) was used to investigate the composition of the as-synthesized products. Ultraviolet−visible (UV−vis) spectrophotometer (UV2700) was used to collect the absorption spectra of the $MAPbI_3$ powder and compounds. Scanning electron microscopy (SEM, FEI Inspect F50) was used to observe the morphology of the products. Transmission electron microscopy (TEM) and HRTEM images were acquired by a FEI G2 20 microscope, with an accelerating voltage of 200 kV. Photoluminescence (PL) spectra and Time-resolved photoluminescence (TR-PL) spectra were obtained on a Fluoromax-4 fluorescence spectrometer (Horiba).

Photoelectrochemical performance tests:

The three-electrode system using a CHI660D electrochemical workstation was used to conduct the Photoelectrochemical performance. The platinum wire was used as the counter electrode, the Ag/AgCl electrode was used as the reference electrode, and the MoC/$MAPbI_3$ modified glassy carbon electrode was used as the working electrode. The frequency was changed from 0.1 to 100 000 Hz to test the electrochemical impedance spectroscopy (EIS), with the AC voltage amplitude at 10 mV. The visible-light source is a 300W Xe lamp equipped with 420 nm filter.

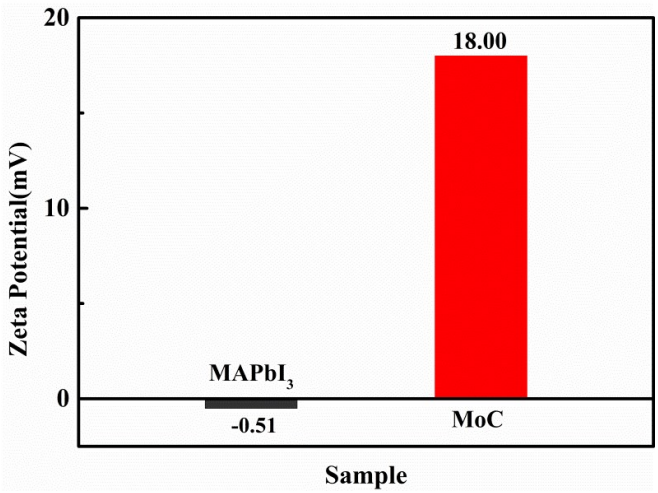

Figure S1. Zeta potentials of $MAPbI_3$ and MoC

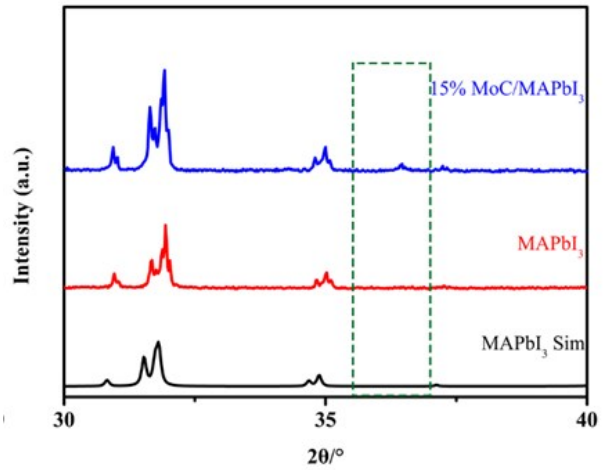

Figure S2. Partial XRD enlarged view of $MAPbI_3$ and MoC/$MAPbI_3$

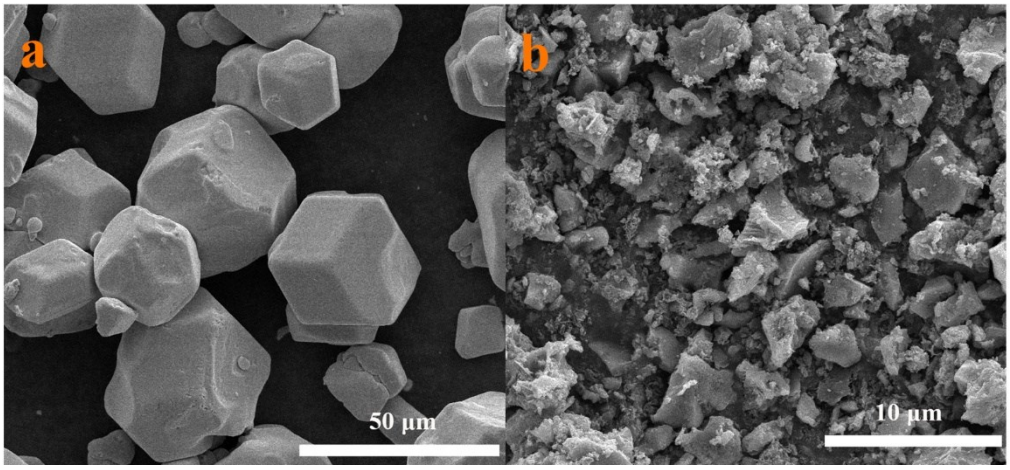

Figure S3. SEM images of a) $MAPbI_3$ and b) MoC

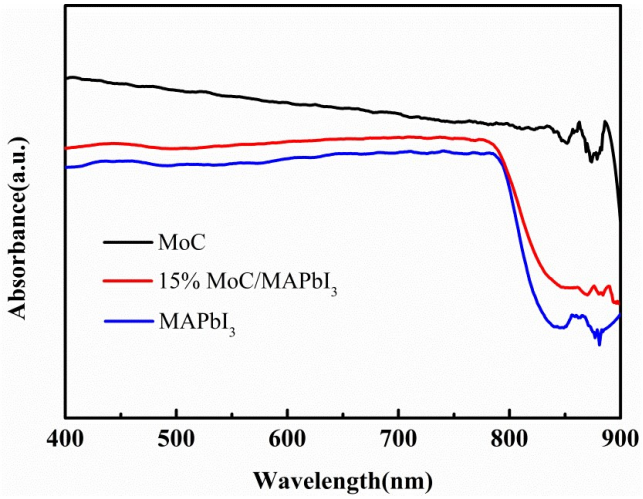

Figure S4. Absorption spectra of MoC, $MAPbI_3$, MoC/$MAPbI_3$

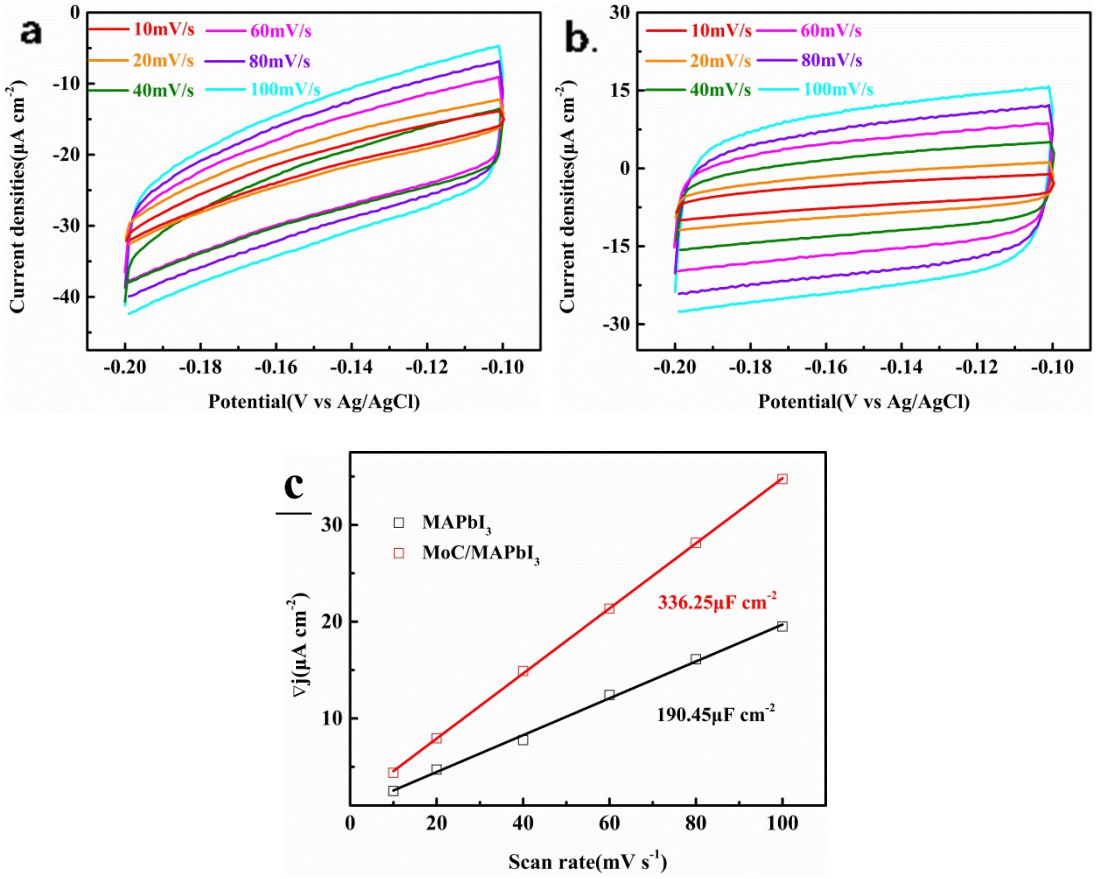

Figure S5. CV curves of $MAPbI_3$ (a) and MoC/$MAPbI_3$ after catalysis (b) tested in the non-faradaic region of -0.2 to -0.1 V vs. Ag/AgCl at various scan rates. (c) The corresponding capacitive currents densities at -0.15 V vs. Ag/AgCl as a function of scan rate.

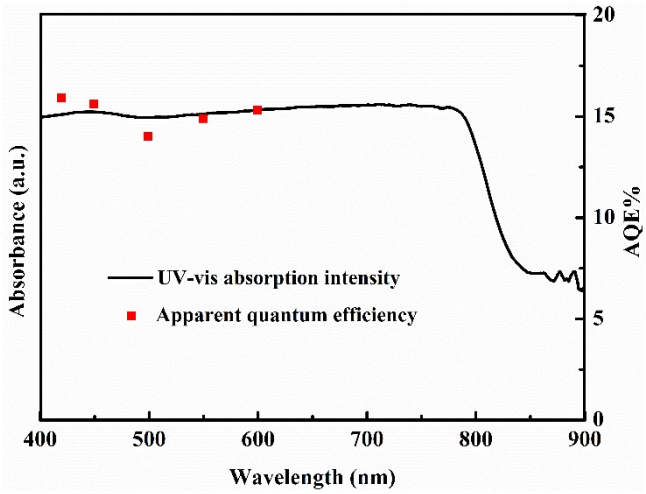

Figure S6. Wavelength dependence of the apparent quantum efficiencies for 15% MoC/$MAPbI_3$.

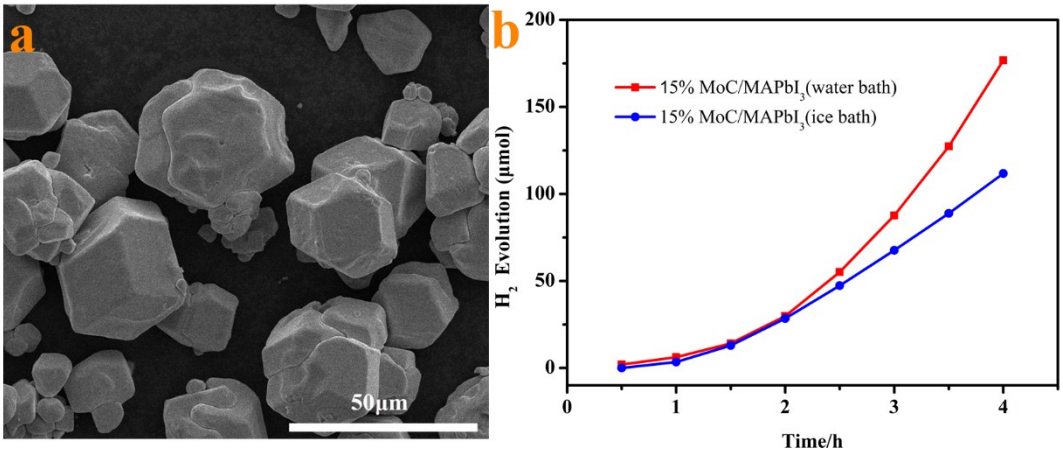

Figure S7. a）SEM image of $MAPbI_3$ synthesis through ice bath and b) comparison of hydrogen production by $MAPbI_3$ with different particle sizes.

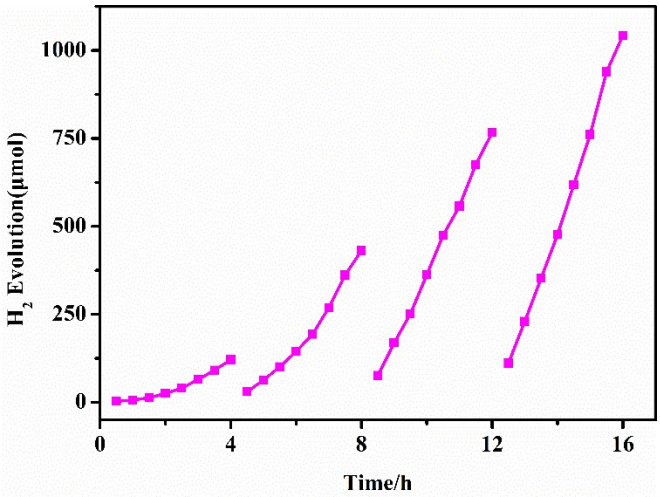

Figure S8. Cycling photocatalytic H_2 evolution performance of the $MAPbI_3$/MoC hybrid of 4 cycles (4 h for each cycle) under visible-light illumination ($\lambda \geqslant$420 nm).

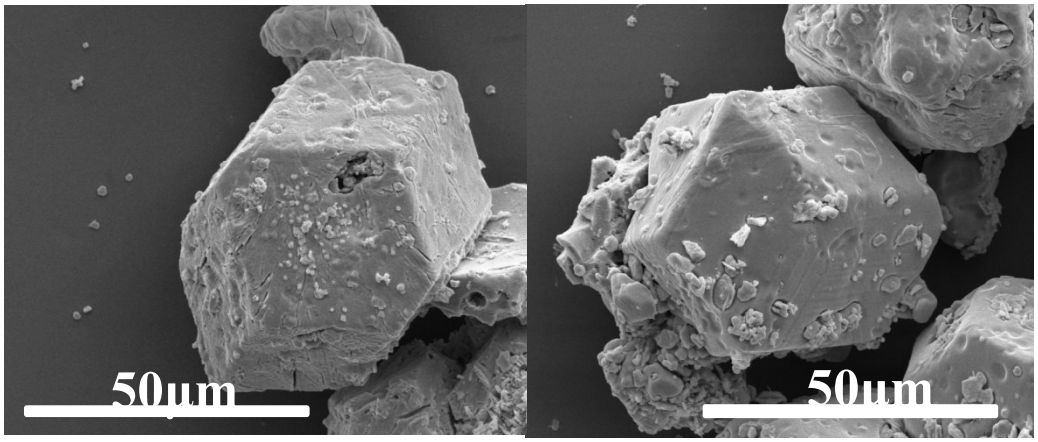

Figure S9. SEM images of MoC/MAPbI$_3$ composites after 16 h photocatalytic reaction

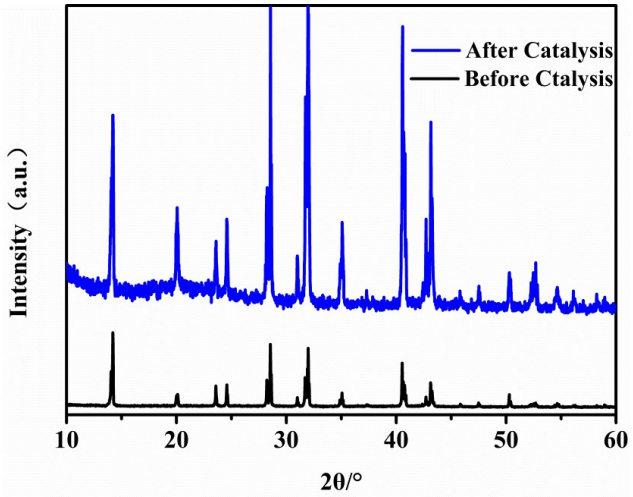

Figure S10. XRD patterns of MoC/MAPbI$_3$ before and after photocatalytic HI splitting reaction

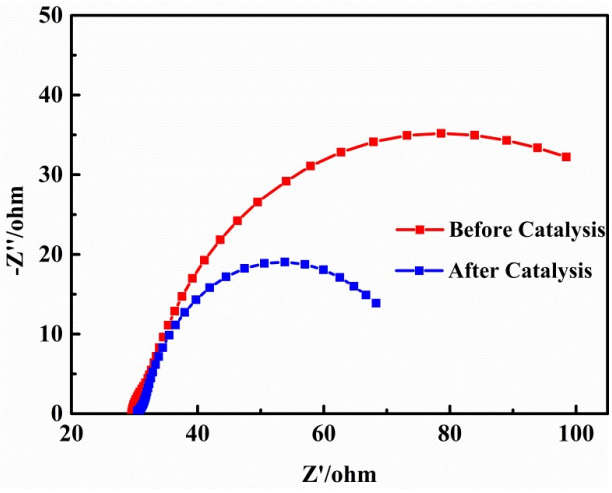

Figure S11. Nyquist plots of 15% MoC/MAPbI$_3$ composites before catalysis and after 16 h catalysis

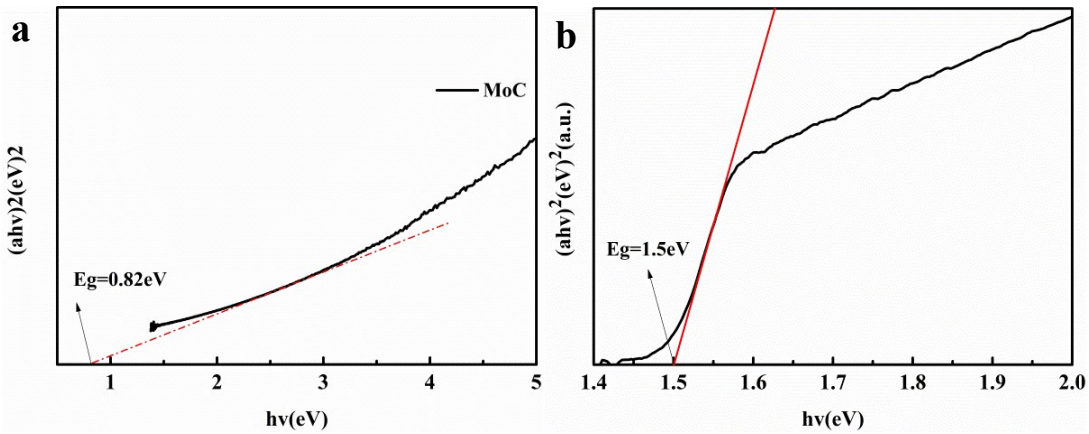

Figure S12. Band gap determination of the a) MoC and b) $MAPbI_3$ powder

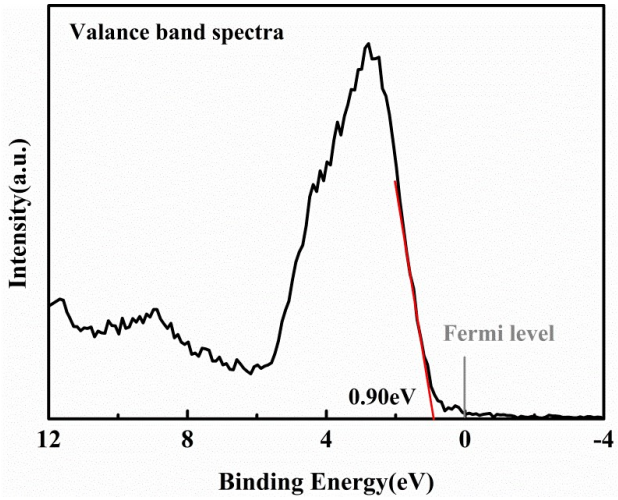

Figure S13. XPS-VB of $MAPbI_3$

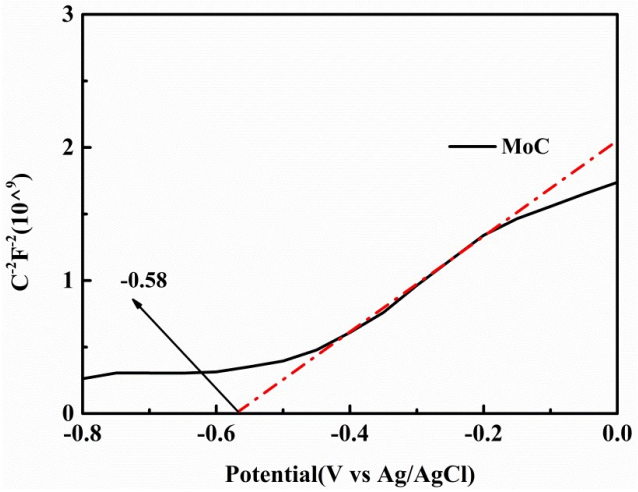

Figure S14. Mott–Schottky plots of MoC

Table S1. Comparison of the fluorescence decay time (τ) and the average lifetime (τ_{avg}) of the $MAPbI_3$ and $MAPbI_3$/MoC hybrid samples.

Catalysts	τ_1 (ns)	B1/%	τ_2 (ns)	B2/%	τ_{avg}(ns)
Pure $MAPbI_3$	0.29	89.28	2.59	10.52	0.490
$MAPbI_3$/MoC	0.39	89.22	6.54	10.78	0.367

Table S2. Comparison of H_2 evolution over reported $MAPbI_3$ in photocatalytic HI splitting system.

Materials	Light source (λ in nm)	H_2 activity ($\mu mol \cdot h^{-1} \cdot g^{-1}$)	Stability (h)	Ref
Pure $MAPbI_3$	300 W Xe lamp (λ ≥ 420 nm)	32.12		**This work**
$MAPbI_3$/Pt	300 W Xe lamp (λ ≥ 420 nm)	86.78		**This work**
$MAPbI_3$/MoC	300 W Xe lamp (λ ≥ 420 nm)	3305.88		**This work**
$MAPb(I_{1-x}Br_x)_3$/Pt	300 W Xe lamp (λ ≥ 420 nm)	2604.8	12	1
$MAPbI_3$/Pt	100W solar simulator (λ > 475nm)	57	160	2
$MAPbI_3$/rGO	300 W Xe lamp (λ ≥ 420 nm)	93.9	200	3
$MAPbI_3$/Pt/TiO_2	300 W Xe lamp (λ ≥ 420 nm)	5293.0	12	4
$MAPbI_3$/Ni_3C	300 W Xe lamp (λ > 420nm)	2362.0	200	5
$MAPbI_3$/CoP	150 W Xe lamp (λ ≥ 420 nm)	2362.0	15	6
$MAPbI_3$/BP	300 W Xe lamp (λ ≥ 420 nm)	3742.0	200	7

$MAPbI_3$/ML-MoS_2	300 W Xe lamp (λ ≥ 420 nm)	13600	208	[8]
$MAPbI_3$/ML-WS_2	300 W Xe lamp (λ ≥ 420 nm)	2380		[8]

1. Y. Wu, P. Wang, Z. Guan, J. Liu, Z. Wang, Z. Zheng, S. Jin, Y. Dai, M.-H. Whangbo and B. Huang, *ACS Catal.*, 2018, **8**, 10349-10357.
2. S. Park, W. J. Chang, C. W. Lee, S. Park, H.-Y. Ahn and K. T. Nam, *Nature Energy*, 2016, **2**, 16185.
3. Y. Q. Wu, P. Wang, X. L. Zhu, Q. Q. Zhang, Z. Y. Wang, Y. Y. Liu, G. Z. Zou, Y. Dai, M. H. Whangbo and B. B. Huang, *Adv. Mater.*, 2018, **30**, 6.
4. X. Wang, H. Wang, H. Zhang, W. Yu, X. Wang, Y. Zhao, X. Zong and C. Li, *ACS Energy Lett.*, 2018, **3**, 1159-1164.
5. Z. J. Zhao, J. J. Wu, Y. Z. Zheng, N. Li, X. T. Li and X. Tao, *ACS Catal.*, 2019, **9**, 8144-8152.
6. C. Cheng, T. Yuan, W. Jian. Hao, L. Jun. Yan, C. Hong. Yan, C. Jing. Hua and K. Dai. Bin, *Advanced Functional Materials*, 2020, *30* (35), 2001478.
7. R. Li, X. Li, J. Wu, X. Lv, Y.-Z. Zheng, Z. Zhao, X. Ding, X. Tao and J.-F. Chen, *Applied Catalysis B: Environmental*, 2019, **259**, 118075.
8. X. L. Zhao, S. Chen, H. J. Yin, S. Y. Jiang, K. Zhao, J. Kang, P. F. Liu, L. X. Jiang, Z. J. Zhu, D. D. Cui, P. R. Liu, X. J. Han, H. G. Yang and H. J. Zhao, *Matter*, 2020, **3**, 935-949.